Chemistry & Biology
Article

A Designed Inhibitor of a CLC Antiporter Blocks Function through a Unique Binding Mode

Andrew E. Howery,[1,2] Shelley Elvington,[1] Sherwin J. Abraham,[1,7] Kee-Hyun Choi,[1,7] Sierra Dworschak-Simpson,[1,7] Sabrina Phillips,[3,7] Christopher M. Ryan,[4,7] R. Lea Sanford,[5,7] Jonas Almqvist,[1] Kevin Tran,[1] Thomas A. Chew,[1] Ulrich Zachariae,[6] Olaf S. Andersen,[5] Julian Whitelegge,[4] Kimberly Matulef,[3] Justin Du Bois,[2] and Merritt C. Maduke[1,*]
[1]Department of Molecular and Cellular Physiology, Stanford University School of Medicine
[2]Department of Chemistry
Stanford University, Stanford, CA 94305, USA
[3]Department of Chemistry and Biochemistry, University of San Diego, San Diego, CA 92110, USA
[4]Pasarow Mass Spectrometry Laboratory, NPI-Semel Institute, David Geffen School of Medicine, University of California Los Angeles, Los Angeles, CA 90095, USA
[5]Department of Physiology and Biophysics, Weill Cornell Medical College, New York, NY 10065, USA
[6]SUPA, School of Physics and Astronomy, University of Edinburgh, Edinburgh EH9 3JZ, UK
[7]These authors contributed equally to this work
*Correspondence: maduke@stanford.edu
http://dx.doi.org/10.1016/j.chembiol.2012.09.017

SUMMARY

The lack of small-molecule inhibitors for anion-selective transporters and channels has impeded our understanding of the complex mechanisms that underlie ion passage. The ubiquitous CLC "Chloride Channel" family represents a unique target for biophysical and biochemical studies because its distinctive protein fold supports both passive chloride channels and secondary-active chloride-proton transporters. Here, we describe the synthesis and characterization of a specific small-molecule inhibitor directed against a CLC antiporter (ClC-ec1). This compound, 4,4'-octanamidostilbene-2,2′-disulfonate (OADS), inhibits ClC-ec1 with low micromolar affinity and has no specific effect on a CLC channel (ClC-1). Inhibition of ClC-ec1 occurs by binding to two distinct intracellular sites. The location of these sites and the lipid dependence of inhibition suggest potential mechanisms of action. This compound will empower research to elucidate differences between antiporter and channel mechanisms and to develop treatments for CLC-mediated disorders.

INTRODUCTION

Small-molecule modulators of ion channels and transporters have a rich history as tools for uncovering mechanisms of ion permeation and as therapeutic agents in the treatment of disease (Gupta, 2011; Yan, 2010). However, the availability of small-molecule modulators and the resulting scientific advances have overwhelmingly favored the broad family of cation-selective channels and transporters. The study of their anion-selective counterparts—and the treatment of diseases related to anion transport (Planells-Cases and Jentsch, 2009; Verkman and Galietta, 2009)—have been hindered by a general lack of anion-transport modulators. Here we describe a new, to our knowledge, small-molecule inhibitor for one family of anion-transport proteins, the CLC "Chloride Channel" family. The availability of such compounds will enable further studies to understand one of the most intriguing aspects of ion transport in the CLC family—the ability of the same general structure to support either passive Cl^- transport or active Cl^-/H^+ antiport. Our findings provide a foundation for the design of new pharmacological agents for studying CLC-mediated physiological processes, including epithelial ion transport, neuronal and skeletal muscle excitability, hippocampal neuroprotection, cardiac pacemaker activity, endocytosis, and lysosomal acidification (Graves, et al., 2008; Huang, et al., 2009; Jentsch, 2008; Jeworutzki, et al., 2012; Lossin and George, 2008; Nighot, et al., 2009; Ratté and Prescott, 2011), and for treating CLC-related disorders, including osteoporosis, neurodegeneration, and cardiovascular disease (Duan, 2011; Jentsch, 2008; Liantonio, et al., 2012; Zhao, et al., 2009).

In expanding the list of CLC modulators, we focused on finding inhibitors of the CLC antiporter from *Escherichia coli*, ClC-ec1 (Dutzler, 2006; Maduke, et al., 1999). We chose this particular protein because it is an excellent structural model for other CLC members (Engh and Maduke, 2005; Estévez, et al., 2003; Lin and Chen, 2003) and it can be produced and purified in large quantities for analysis by multiple biophysical and biochemical techniques. To date, the only known small-molecule inhibitor of a CLC antiporter was 4,4′-diisothiocyano-2,2′-stilbenedisulfonic acid (DIDS) (Matulef and Maduke, 2005), which inhibits many different transporters and channels. DIDS is of limited practical utility because of its low-affinity, promiscuous binding (Cabantchik and Greger, 1992) and instability in aqueous solution (Jakobsen and Horobin, 1989). This instability leads to the formation of polythiourea compounds, which are more stable than DIDS and are more potent inhibitors of ClC-ec1 (Matulef, et al., 2008). These compounds, however, possess two major disadvantages that limit their usefulness. First, they are large,

conjugated molecules that are impractical to synthesize and modify for structure-activity investigations. Second, the polythiourea inhibitors cause aggregation of detergent-solubilized protein, thus precluding crystallographic or spectroscopic characterization of the binding site. Here, we introduce a new, to our knowledge, ClC-ec1 inhibitor design, 4,4'-octanamidostilbene-2,2′-disulfonate or "OADS," and provide a comprehensive series of experiments to elucidate the details of its molecular interactions with the protein.

In the context of the CLC family, OADS offers a unique opportunity to study differences and similarities between two major classes of membrane proteins. Although CLCs originally were thought to be solely voltage-gated Cl^- channels, many are Cl^-/H^+ antiporters (Accardi and Miller, 2004; Picollo and Pusch, 2005; Scheel, et al., 2005). Selective CLC inhibitors thus offer the potential to become tools to probe how these two ostensibly different ion transport processes can be supported by closely related protein structures (as deduced by sequence similarity together with compelling structure-function analyses) (Engh and Maduke, 2005; Estévez, et al., 2003; Lin and Chen, 2003; Lísal and Maduke, 2009; Miller, 2006). The classic "chloride-channel inhibitors" have broad specificity, inhibiting many types of Cl^- channels and transporters, and even cation channels (Alper, 2009; Chen, et al., 2007; Evanko, et al., 2004; Kasai, et al., 1999; Li, et al., 2008). OADS is highly effective against the Cl^-/H^+ antiporter ClC-ec1 but has little activity against a CLC from the channel branch of the family, suggesting that the differences between permeation and active transport may be teased apart using molecular probes. To our knowledge, OADS also is the first inhibitor of the CLC antiporters that is reversible, has low molecular weight (<1000 Da), and is amenable to structural modification. We capitalize on these properties to characterize inhibitor binding, thus providing a basis for developing future generations of CLC-specific inhibitors that eventually may have therapeutic application in treating osteoporosis and neurodegenerative and cardiovascular diseases (Duan, 2011; Liantonio, et al., 2012; Zhao, et al., 2009).

RESULTS

Chemical Combination of Generic Cl^--Channel Inhibitors Yields a Potent CLC Antiporter Inhibitor

In our search for modulators of CLC function, we tested known CLC channel inhibitors as lead compounds. This panel included flufenamic acid, the clofibric acid derivative 2-(p-chlorophenoxy)-3-(4-chlorophenyl)propionic acid, 9-anthracene carboxylate (9AC), 5-nitro-2-(3-phenylpropylamino)benzoic acid (NPPB), niflumic acid, octanoic acid, and 4,4'-diaminostilbene-2,2′-disulfonate (DADS) (Estévez, et al., 2003; Gradogna and Pusch, 2010; Venglarik, et al., 1994; Zhang and Chen, 2009). None of these compounds inhibited ClC-ec1; however, a modified compound (OADS) combining DADS with two aliphatic side chains mimicking the hydrophobic element of octanoic acid (Figure 1A) inhibited ClC-ec1 at low-micromolar concentrations.

We first assessed OADS' inhibition of ClC-ec1 using a Cl^- efflux assay (Walden, et al., 2007), where ClC-ec1 is reconstituted into liposomes containing a high internal chloride concentration relative to the extraliposomal buffer, and activity is measured as the rate at which the protein passes Cl^- along this steep concentration gradient (Figure 1B). OADS inhibited ClC-ec1 with a concentration for half-maximal inhibition (K_i) of 29 μM (Figure 1C, black circles), whereas neither parent compound detectably inhibited ClC-ec1 (Figure 1C, blue circles and triangles) at concentrations up to 1 mM (not shown). Thus, the chemical combination of two conventional Cl^- channel inhibitors (octanoic acid and DADS) results in an increase in potency compared to either parent compound by well over 100-fold.

We also examined ClC-ec1 inhibition by OADS using bilayer recordings, which allow for precise control of transmembrane voltage and solutions on both sides of the membrane (Miller, 1983). In these experiments, ClC-ec1-reconstituted liposomes were fused to planar lipid bilayers, and the ionic currents carried by ClC-ec1 were measured under voltage clamp. OADS was then perfused onto one side of the bilayer, and the degree of inhibition was recorded (Figure 1D). We observe maximal inhibition of ~40% when OADS is added to the *cis* chamber (Figure 1E). Because CLC-ec1 inserts into bilayers with random orientation (Matulef and Maduke, 2005) and OADS is a side-specific inhibitor (as shown below), the maximal inhibition possible in these experiments is ~50%. In contrast, in the Cl^- efflux assays, OADS is allowed access to both sides of the membrane through freeze fracture of liposomes during their preparation, thereby allowing nearly complete inhibition (Figure 1C). In bilayers, the modest increase in potency from K_i ~3.6 μM at +100 mV to ~2.7 μM at −100 mV (Figure 1E) is consistent with the negatively charged inhibitor sensing part of the transmembrane electric field on its way to the inhibitory binding site (Woodhull, 1973). Inhibition by OADS is completely reversible within 4–10 min (with 4 min being the minimum amount of time required for full solution exchange of the bilayer chamber) (Figure 1F).

The K_i values measured in bilayers (~3 μM, Figure 1E) are an order of magnitude lower than the values determined using the Cl^- efflux assay (~30 μM, Figure 1C, black circles). Given the sensitivity of ClC-ec1 activity to membrane composition (Robertson, et al., 2010) (Figure S1 available online), we hypothesized that the different K_i values could be due to the presence of an additional negatively charged lipid (cardiolipin) in the *E. coli* lipid extract used for the efflux assays, which was not present in the bilayer experiments. To test whether the presence of cardiolipin (CLN) affects OADS potency, we did Cl^- efflux assays on ClC-ec1 reconstituted into liposomes composed of a defined lipid mixture identical to that used in the bilayer experiments (with phosphatidylethanolamine [PE] and phosphatidylglycerol [PG] head groups and lacking CLN) (PE/PG liposomes). Consistent with our hypothesis, the change in lipid composition decreased K_i from 29 to 7.3 μM, (Figure 1G, triangles), close to that observed in the planar bilayer experiments. Substituting CLN for PG restores the K_i to that observed in the original *E.coli* polar lipid liposomes (Figure 1G, blue and black circles). These data indicate that inhibition of ClC-ec1 by OADS is sensitive to the lipid bilayer composition.

OADS Effect on Protein Activity Is Not Solely Mediated by Bilayer Modification

With a K_i as low as 3 μM (in PE/PG membranes, Figure 1E), OADS is among the most potent CLC inhibitors, as well as the only well-behaved small-molecule inhibitor of any CLC antiporter. But the dependence of ClC-ec1 activity and OADS

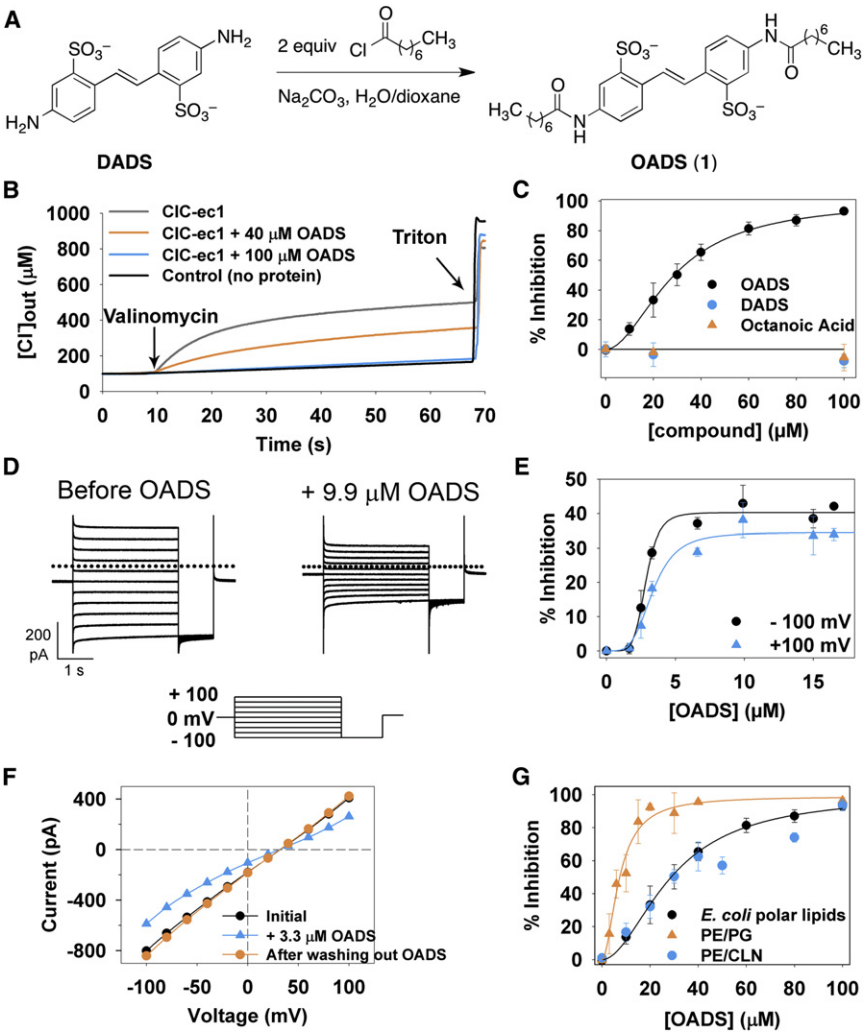

Figure 1. OADS Is a CLC Antiporter Inhibitor

(A) Synthesis of OADS from the generic chloride channel inhibitors octanoic acid and DADS.

(B) Raw data from Cl^- efflux assays. ClC-ec1 is reconstituted into liposomes, and efflux is initiated by the addition of valinomycin; Triton X-100 is added at the end of each experiment to release all of the chloride from the liposomes (see Experimental Procedures for more details).

(C) Concentration dependence of ClC-ec1 inhibition in Cl^- efflux assays. Each data point represents the mean inhibition ± standard error of the mean (SEM) for three to seven experiments at each concentration. For OADS, the solid line is a fit of the data to the equation: $I = (I_{max} \times [OADS]^n)/(K_i^n + [OADS]^n)$, where I is the percentage inhibition, I_{max} is the maximal inhibition, K_i (29 μM) is the apparent affinity, and n (1.9) is the Hill coefficient.

(D) Currents carried by ClC-ec1 in planar lipid bilayers in response to the voltage protocol shown below before (left) and after (right) addition of 9.9 μM OADS to one side (the *cis* chamber) of the bilayer.

(E) Concentration dependence of the inhibition by OADS in bilayers. Each data point represents the mean inhibition ± SEM from three to seven bilayers with OADS added to the *cis* chamber. At +100 mV, I_{max} = 34%, K_i = 3.4 μM, and n = 3.9. At −100 mV, I_{max} = 40%, K_i = 2.9 μM, and n = 6.1.

(F) Reversibility of OADS inhibition in bilayers. Current-voltage curves before (black) and after adding 3.3 μM OADS to the *trans* chamber (blue squares), and after perfusion with OADS-free solution (red triangles). Similar results were obtained with two other bilayers, and in all cases reversal was complete within 4–10 min (with 4 min being the minimum amount of time required for full perfusion).

(G) Effect of liposome composition on ClC-ec1 sensitivity to OADS in Cl^- efflux assays. Data for *E. coli* polar lipids are identical to those in panel (C). For PE/PG liposomes, K_i = 7.3 μM and n = 1.9; for PE/CLN, K_i = 32 μM and n = 1.5.

See also Figures S1 and S4.

potency on bilayer composition (Figure 1G; Figure S1) raises the question as to whether the inhibition results from a specific interaction with the protein, from a more general modification of the lipid bilayer, or from some combination of these mechanisms (Figure 2A).

To address these questions, we employed an assay that exploits gramicidin channels to distinguish between inhibition that occurs solely through modification of bilayer properties and inhibition that involves a direct effect on the protein (Figure 2B). Briefly, the sensitivity of gramicidin channel activity to lipid bilayer properties (Lundbaek, et al., 2010) is used to report on bilayer modification by an exogenously added compound (Ingólfsson and Andersen, 2010). On its own, a positive result in the gramicidin assay may not be remarkable because many druglike compounds are amphiphiles. Such compounds will therefore also have bilayer modifying activity (at some concentration) in addition to their target-specific activity. The power of the assay lies in its application to a panel of (related) compounds. If a compound inhibits activity of a membrane protein target solely through a bilayer-modification mechanism, the target-specific and the bilayer effects should occur at similar concentrations; moreover, the bilayer-modifying potency of a panel of related compounds will be positively correlated with their relative inhibitory potency. Conversely, if the compound has specific interactions with the target, the relative inhibitory potency for the set of compounds will deviate from such a correlation (Ingólfsson and Andersen, 2010). To implement this analysis, we synthesized and tested a panel of OADS derivatives (Figures 2C–2E). There is an unmistakable break in the correlation between the two assays: the *cis* isomer of OADS is several-fold less potent against ClC-ec1 than its *trans* counterpart (Figure 2D), yet it is the more potent bilayer-modifying compound (Figure 2E). Thus, inhibition is not solely due to a modification of bilayer properties (mechanisms 4 and 5 in Figure 2A), but rather the predominant mechanism of OADS inhibition of ClC-ec1 occurs through specific interactions with the protein (mechanisms 1, 2, or 3 as in Figure 2A).

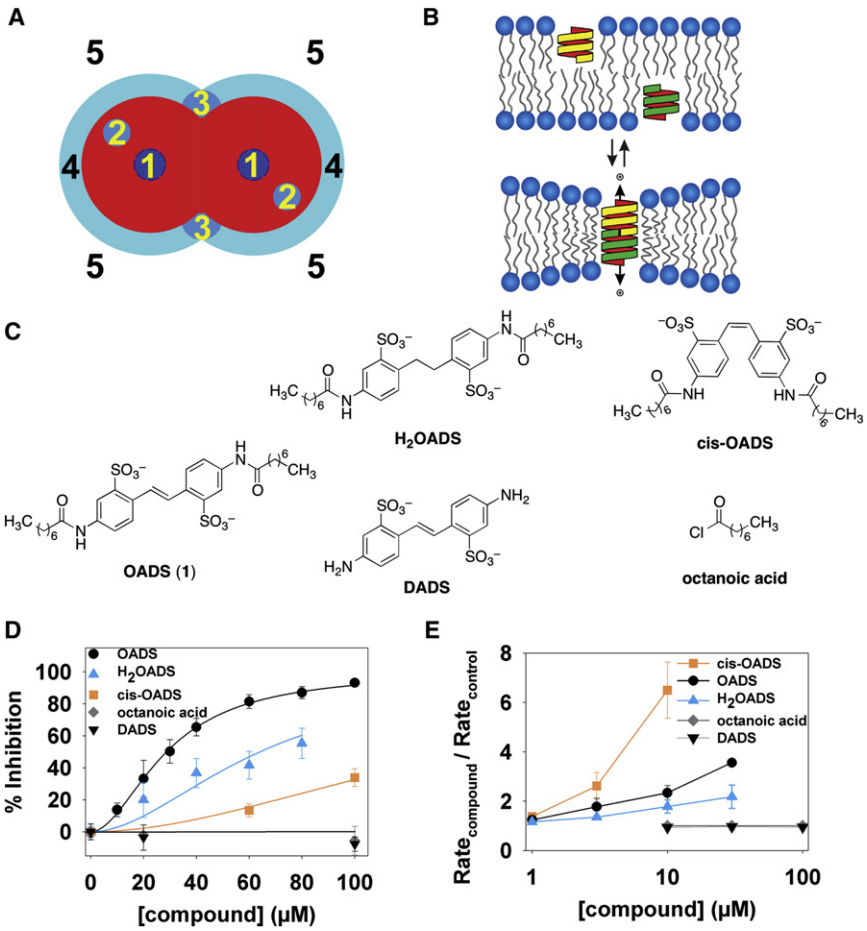

Figure 2. Inhibition of ClC-ec1 by OADS Results Predominantly from Drug-Protein Interactions

(A) Mechanisms by which drugs can inhibit transporter function: (1) Occluding the transport path to block ion movement; (2) binding to sites formed by the protein, to alter function by altering the free energy difference between different conformations; (3) binding to selective sites at the protein/bilayer interface, which may also alter the bilayer deformation energy contribution to the free energy difference between different conformations; (4) nonspecific accumulation at the protein/bilayer interface to alter the local lipid packing; and (5) partitioning at the bilayer/solution interface to alter lipid bilayer material properties, which both will alter the bilayer contribution to the membrane protein's conformational equilibrium (Modified after Andersen, 2008).

(B) Changes in bilayer properties can be determined by measuring changes in the gramicidin (gA) monomer↔dimer equilibrium (e.g., Lundbaek, et al., 2010) because the hydrophobic length of the bilayer-spanning, ion conducting, dimeric gA channel is less than the hydrophobic length of the host bilayer. gA channel formation therefore leads to a local membrane thinning, with an associated energetic cost that varies with changes in the bilayer properties, thus making gA channels suitable probes for changes in bilayer properties.

(C) Panel of OADS derivatives tested for ClC-ec1 potency and bilayer modification: OADS, *cis*-OADS, H_2OADS, DADS, and octanoic acid.

(D) Dose-response curves for inhibition of ClC-ec1 activity by OADS derivatives, as determined by Cl^--efflux assays on liposomes formed from *E. coli* polar lipids (as in Figures 1B and 1C). Each data point represents the mean inhibition ± SEM for three to five experiments at each concentration, with the exception of H_2OADS points, which represent the average of two experiments ± range.

(E) Dose-response curves for the OADS derivatives' effects on bilayer properties, as reported by increases in gA activity. gA activity is determined from the time course of Tl^+-induced quenching of a fluorophore encapsulated in gA-doped large unilamellar liposomes (see Experimental Procedures for more details). The quench rate in the presence of a compound normalized to the rate in the absence of added compound reflects the degree of bilayer modification (Ingólfsson and Andersen, 2010).

OADS Selectively Inhibits the CLC Antiporter ClC-ec1 over the CLC Channel ClC-1

Having established that OADS inhibits ClC-ec1 through specific interactions with the protein, we next sought to address whether OADS (like other stilbene derivatives) also acts as a broad-spectrum inhibitor of chloride channels or whether it displays selectivity toward the chloride-proton antiporter ClC-ec1. OADS was tested for activity against the CLC chloride channel ClC-1 using inside-out patches excised from *Xenopus* oocytes expressing human ClC-1. As shown in Figures 3A and 3C, 30 μM OADS (which inhibits ClC-ec1 by 84% in PE/PG liposomes) inhibits ClC-1 by only 20%. This low potency of OADS toward ClC-1 could be solely due to the lipid composition of the oocyte membrane, given the previously noted influence of lipids on inhibition by OADS (Figure 1). Accordingly, it is informative to compare the *cis* and *trans* isomers of OADS within each environment. In contrast to inhibition of ClC-ec1, similar degrees of ClC-1 inhibition are observed with both *cis* and *trans* OADS isomers (Figures 3B and 3C). This result suggests that the *cis* isomer of OADS acts through a more generic mechanism (such as bilayer modification, as discussed above), whereas the *trans* isomer ("OADS", Figure 2B) acts through more specific molecular contact with ClC-ec1.

OADS Binds to and Inhibits ClC-ec1 with a 2:1 Stoichiometry

In the chloride efflux assays, the inhibition curves are best fit with a Hill coefficient of 1.9, which suggests that ClC-ec1 inhibition requires at least two OADS to bind per protein subunit (Figure 1C). ClC-ec1 is a homodimer, with each monomer acting as an independent transporting unit (Robertson, et al., 2010). In bilayer recordings, the Hill coefficient for OADS inhibition ranges from 3.9 at +100 mV to 6.1 at −100 mV (Figure 1E). Given that OADS has some bilayer-modifying activity (Figure 2D), the larger Hill coefficient in the latter experiments could be due to OADS interacting with the bilayer and not directly with the protein. To focus on the protein-specific aspect of OADS binding to and inhibition of ClC-ec1, we investigated the covalent binding of a photoreactive OADS derivative with detergent-solubilized protein. Covalent modification of ClC-ec1 by this reagent allows

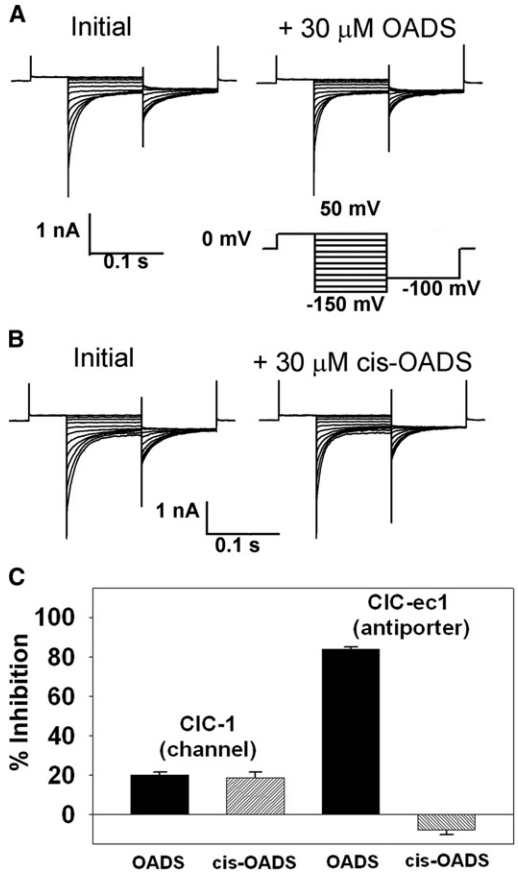

Figure 3. OADS Is a Selective CLC Inhibitor

(A) Representative current families from inside-out patches excised from *Xenopus* oocytes expressing human ClC-1. Currents before (left) and after (right) steady-state inhibition in 30 μM OADS were elicited by the voltage protocol shown below the traces.

(B) ClC-1 currents as in (A) but with 30 μM *cis*-OADS.

(C) Summary data comparing inhibition of ClC-1 by OADS and *cis*-OADS (left) to inhibition of ClC-ec1 by OADS and *cis*-OADS (right). ClC-ec1 was reconstituted in PE/PG liposomes and measured in Cl^- efflux assays. For each experiment, data represent the mean ± SEM for three experiments.

for use of mass spectrometry to identify the number of OADS molecules bound per protein subunit. By quantifying the Cl^- flux activity of the modified protein, we then could determine how many bound OADS molecules are necessary and sufficient for inhibition.

To synthesize an OADS analog suitable for photoaffinity labeling, we chose a diazirine photophore, because this functional group only slightly perturbs the OADS structure, its photoactivation generates an electrophilic carbene that can react with any nearby C–H, N–H, or O–H bond, and it is activated at 365 nm, a wavelength that will not induce photolytic protein damage (Dormán and Prestwich, 2000). The synthesis of a diazirine-OADS photoaffinity-labeling reagent ("PAL-OADS") is shown in Figure S2A. The K_i of PAL-OADS for ClC-ec1 is 80 μM, as determined by the Cl^- efflux assay in *E. coli* polar lipids (Figure S2B), a 2- to-3-fold increase compared to OADS (Figure 1C).

In liposomes, irreversible inhibition by PAL-OADS was observed only when the sample was irradiated with 365-nm light, thus confirming that PAL-OADS acts as a light-dependent covalent inhibitor (Figure S2C). To quantify the relationship between photo-incorporation and inhibition, solubilized ClC-ec1 was incubated with PAL-OADS and irradiated with 365 nm light. These samples were then split into aliquots for either analysis by mass spectrometry or reconstitution into liposomes for activity analysis (Figures 4A–4C). The sample labeled with the lower concentration of PAL-OADS showed no inhibition relative to unmodified ClC-ec1, though 40% of the protein was modified by a single OADS molecule (Figure 4C, middle); this result indicates that binding of one equivalent of OADS per ClC-ec1 is not sufficient to inhibit function. The sample labeled with the higher concentration of PAL-OADS (400 μM) was inhibited 62% (Figure 4C, right), which best correlates to the amount of protein that is at least doubly labeled (44%), but not to the amount that is triply labeled (10%). These results are consistent with the Hill coefficient of ~2 determined in the Cl^- efflux assays (Figure 1B) and demonstrate that the binding of two OADS molecules per subunit is necessary and sufficient for inhibition.

Inhibition by OADS Is Mediated by Binding to Two Distinct Intracellular Sites

Having established that direct binding of OADS to ClC-ec1 is responsible for inhibition, we sought to obtain structural details of the inhibitor-binding sites. ClC-ec1 crystals grown in the presence of (or soaked with) OADS failed to reveal density corresponding to the small molecule. An alternative strategy using PAL-OADS in combination with "top-down" mass spectrometry (MS) was, therefore, explored (Robinette, et al., 2006). Top-down MS uses high-resolution Fourier-transform mass spectrometry to measure the intact mass of the protein in combination with fragmentation either by collisionally activated or electron-capture dissociation (CAD/ECD), producing product ions for tandem mass spectrometry whose masses are sequence and modification specific (Kelleher, 2004). Analysis of the single-labeled protein revealed a binding site localized within residues 109 and 185 of ClC-ec1; analysis of the double-labeled protein revealed a second locale within the first 40 residues of the N terminus (Figure 5A; Figure S3; Tables S1 and S2).

The MS data show that both OADS-binding sites are localized to the intracellular side of the membrane. This result cannot be compared directly with our functional assays because reconstituted ClC-ec1 adopts mixed orientations in liposomes and bilayers. We can achieve "functional orientation," however, by taking advantage of the fact that DIDS inhibits ClC-ec1 specifically from the intracellular side, as demonstrated in bilayer recordings (Matulef and Maduke, 2005). Figure 5B shows a schematic representation of transporters oriented within a bilayer in opposite directions relative to the two bilayer chambers (called *cis* and *trans*). If OADS inhibits exclusively from the intracellular side, the addition of OADS to the *cis* chamber after addition of DIDS to the same chamber should have no further effect (Figure 5B, case 1). In contrast, if OADS inhibits from the extracellular side, the addition of OADS to the *cis* chamber after addition of DIDS to the same chamber should cause further inhibition (Figure 5B, case 2). We observe that application of OADS following addition of DIDS to the same chamber has no effect, consistent with Case 1 (Figure 5C). Likewise, the application of DIDS following addition of OADS to the same chamber has no

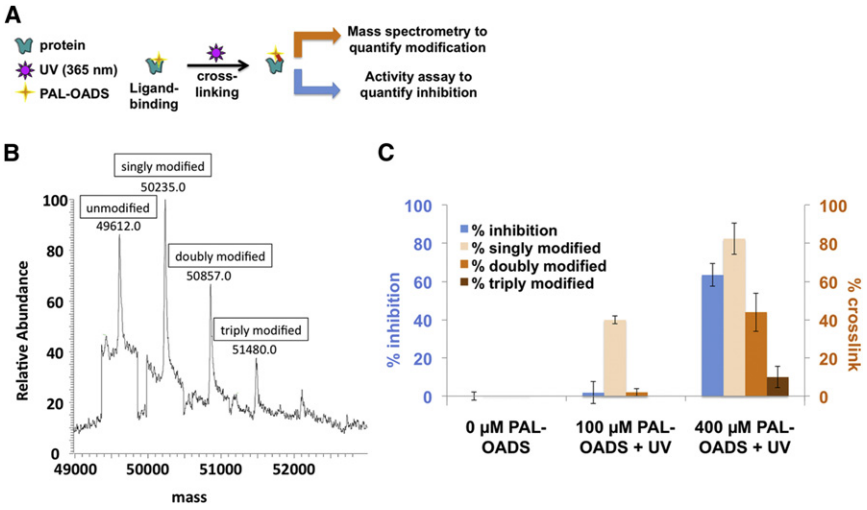

Figure 4. Binding Two Molecules of OADS per ClC-ec1 Protein Subunit Is Necessary and Sufficient to Inhibit ClC-ec1 Function

(A) Experimental schematic: cross-linked protein was subjected to mass spectrometry analysis, as in (B), and functional studies (reconstitution and Cl^-- efflux assays, as in Figures 1B and 1C).

(B) Covalent modification of ClC-ec1 with 400 μM PAL-OADS detected by mass spectrometry.

(C) Comparison of percentage of inhibition of ClC-ec1 activity measured using Cl^- efflux (blue bars) to percentage of ClC-ec1 that is singly, doubly, and triply modified (light orange, medium orange, and brown bars, respectively). ClC-ec1 in the presence of 0, 100, or 400 μM PAL-OADS was irradiated with 365 nm light UV and then split into two samples as illustrated in panel (A). "Singly modified" corresponds to percentage of ClC-ec1 covalently linked to at least one equivalent of PAL-OADS (sum of singly, doubly, and triply modified protein), detected by mass spectrometry as in panel (B). "Doubly modified" corresponds to percentage of ClC-ec1 covalently linked to at least two equivalents of PAL-OADS (sum of doubly and triply modified protein). "Triply modified" corresponds to percentage of ClC-ec1 covalently linked to three equivalents of OADS. The combined results demonstrate that (1) binding of one OADS molecule to ClC-ec1 does not inhibit ClC-ec1 (middle, results with 100 uM PAL-OADS), (2) binding of two OADS molecules correlates well with inhibition (right, results with 400 μM PAL-OADS), and (3) binding of three OADS molecules is not required for inhibition (right, results with 400 μM OADS). Results represent the mean of three experiments (±SEM). See also Figure S2.

effect (Figure S4A). In further support of this model, the application of OADS to the opposite chamber from DIDS results in significant additional inhibition (Figures S4B and S4D), as does application of DIDS to the opposite chamber from OADS (Figures S4C and S4D). Hence, OADS inhibits ClC-ec1 from the intracellular side, in agreement with the mass spectrometry results.

To confirm and further refine the location of the OADS-binding sites, we tested the functional effect of mutations in each of the regions identified through mass spectrometry. We targeted cationic amino acid residues, reasoning that neutralization of such residues near the binding pockets would decrease affinity of the dianionic OADS molecule. Figure S5 shows a summary of the mutations that had no (or very little) effect on K_i for OADS. Of the residues tested, two sites were found in which neutralization disrupted OADS inhibition. Within the first region identified by MS (residues 109–185; Figure 5A), the K169A mutant exhibited a 2-fold decrease in sensitivity to OADS (K_i = 68 μM), whereas mutating the three nearby arginine residues (R160, R167, and R174, located within 5 Å of K169) had no influence (Figure 6A; Figure S5A). This result indicates that a mutation at K169 changes OADS affinity through disruption of a specific interaction rather than through a more general electrostatic effect. Within the second region identified by MS (residues 15–40; Figure 5A), we found that R28A in combination with K216A (which is within 9 Å in 3-dimensional space) eliminated all detectable inhibition in PE/PG lipids (Figure 6B) and reduced the inhibition in *E. coli* lipids several fold (Figure 6A). The residual inhibition in *E. coli* lipids is similar to the inhibition observed with *cis*-OADS (Figure 6C). K_i values could not be determined for the R28A/K216A mutant because of the solubility limit of OADS (100 μM). This decrease in OADS affinity for mutant ClC-ec1 is specific to R28/K216, as mutation of R23 and K30 or R17, R18, and R19 had no effect on OADS inhibition (Figure S5).

Simulations of OADS:ClC-ec1 Binding in a Lipid Bilayer

We also studied the binding of OADS to ClC-ec1 by atomistic molecular dynamics simulations in POPE/POPG (3:1) membranes, which were done without prior knowledge of any experimental data concerning the OADS binding sites. Figure 7A shows the simulation system. In five simulations (each 30–85 ns, with a total simulation time of 265 ns), six to eight OADS molecules were inserted in the aqueous phase near the membrane. Most OADS molecules rapidly moved to the membrane/solution interface (not all molecules had entered the interfacial region at the time the snapshot in Figure 7A was taken), with the OADS sulfate groups interacting with the phospholipid head groups. Contacts between OADS and K169 were observed in two simulations; contacts between OADS and the region near R28 and K216 were observed in three simulations. Both interactions were observed in one simulation, where two OADS molecules associated with the intracellular side of ClC-ec1: one of them formed a tight ionic interaction between K169 and the anionic sulfate on OADS; the second interacted with a larger region of the adjoining ClC-ec1 subunit near K216 and R28, involving a contact to the backbone of R28 (Figures 7B and 7C). The limited timescale of the simulations does not allow conclusions about the thermodynamic stability of these binding modes, but the results lend further support to our experimental data implicating K169 and R28/K216 as specific, functionally relevant sites of OADS binding to ClC-ec1.

DISCUSSION

Despite recent progress in the generation of CLC-specific inhibitors of certain homologs, including a scorpion venom toxin specific for ClC-2 (Thompson, et al., 2009) and small-molecule inhibitors of the ClC-K channels (Gradogna and Pusch, 2010; Liantonio, et al., 2008), the CLCs lack the extensive array of

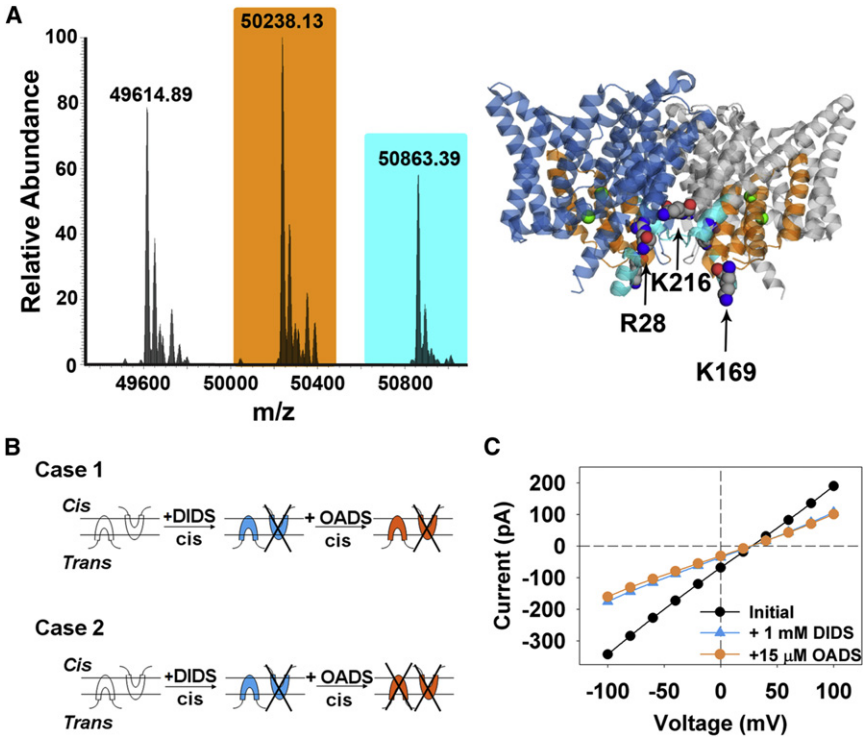

Figure 5. Binding and Inhibition by OADS Occurs at Two Distinct Intracellular Sites

(A) "Top-down" mass spectrometry was used to identify the OADS-binding regions in ClC-ec1. The ClC-ec1 structure illustrates the identified region of labeling of the singly modified protein in orange (residues 109–185) and an additional site identified in the doubly modified protein in cyan (residues 15–40). The singly modified protein was modified only at the 109–185 site and not at the 15–40 site; the doubly modified protein was modified at both locations. The two subunits are depicted in blue and gray, and Cl^- ions are space-filled in green.

(B) Schematic cartoons depicting side-specific inhibition of ClC-ec1 by OADS. ClC-ec1 protein is randomly oriented in bilayers. Case I shows that if OADS, like DIDS, acts from the intracellular side, adding OADS to the *cis* chamber after addition of DIDS will have no effect. Case 2 shows that if OADS acts from the extracellular side, adding OADS to the *cis* chamber after addition of DIDS should cause further inhibition.

(C) Current-voltage curves obtained in bilayer recording experiments before (black circles) and after adding 1 mM DIDS to the *cis* chamber (blue triangles), and after subsequent addition of 15 μM OADS to the *cis* chamber (orange circles). That no additional inhibition was observed upon addition of OADS is consistent with Case 1, with OADS inhibition occurring at the intracellular side of ClC-ec1. See also Figures S3 and S4 and Tables S1 and S2.

small-molecule modulators available for other membrane proteins. We have developed and characterized a novel CLC inhibitor, "OADS" which, to our knowledge, is the first small-molecule inhibitor of CLC antiporters that is of sufficient affinity and stability to be used in both functional and biochemical studies. OADS was created through the combination of two generic chloride-channel inhibitors, each of which shows no efficacy against ClC-ec1. The maximal observed affinity of OADS for ClC-ec1 (K_i ~3 μM) is well within the range of typical lead compounds, and we anticipate that further iterative modification (performed in tandem with functional studies), will result in improved next-generation inhibitors that will facilitate atomistic studies of these important membrane proteins.

The information we have gathered on OADS binding and inhibition of ClC-ec1 provide insight into possible mechanisms of inhibition. Functional and mass spectrometric analysis of the singly modified protein (Figures 4C and 4D) shows that binding at a single site between residues 109 and 185 occurs first (because no modification at the second site is observed in the singly modified protein.) This site involves K169, as evident from our mutational (Figures 6A, 6C, and 6D) and modeling (Figures 7B and 7C) studies. However, binding to this site alone is not sufficient to inhibit function; inhibition is observed only when OADS is bound to two discrete locations (Figure 4D). Because binding to the second (R28/K216) site is not observed in the absence of binding to the K169 site (Figure 5A), we conclude that binding of OADS at the K169 site is required for binding to the second site.

Mutating R28 and K216 to alanine eliminates all detectable inhibition of ClC-ec1 reconstituted in PE/PG and decreases inhibition in *E. coli* lipids several fold (Figures 6A and 6B). The residual inhibition in *E. coli* lipids may be due to nonspecific bilayer effects, rather than specific OADS-protein interactions. The magnitude of such an effect is likely to depend on the bilayer composition, which could account for the differences between the inhibition observed in PE/PG versus *E. coli* lipids. Nonspecific binding, however, cannot be the primary mechanism of action of OADS on the wild-type protein (as discussed above, Figure 2), but may account for the residual inhibition observed in the R28A/K216A mutant. In support of this hypothesis, *cis*-OADS (which is more bilayer-modifying but a less effective inhibitor of wild-type ClC-ec1; Figures 2D, 2E, and 3C) inhibits the R28A/K216A mutant with similar potency to the *trans*-OADS isomer (Figure 6C). Likewise, ClC-1 (which lacks positively charged residues at the corresponding positions) is inhibited only 20% by OADS, and is equally inhibited by both the *cis* and *trans*-OADS isomers (Figure 3). Together, these data further support our model for specific OADS-R28/K216 interactions in the inhibition of ClC-ec1 and illustrate the importance of testing for bilayer effects.

Does OADS inhibit eukaryotic CLC antiporters? Addressing this question is challenging given the low currents exhibited by eukaryotic CLCs in inside-out patches and the fact that eukaryotic CLCs have not been functionally reconstituted for use in either bilayer recordings or efflux assays. Sequence alignments around the regions that contribute to OADS potency in ClC-ec1 are too wobbly to reliably predict which homologs contain positively charged residues in positions equivalent to R28, K169, and K216 (and thus to predict which homologs are sensitive to OADS). Nevertheless, it is intriguing that, in some alignments, position 169 (at the site of initial binding) contains a positively charged residue in most CLC antiporters and a negatively

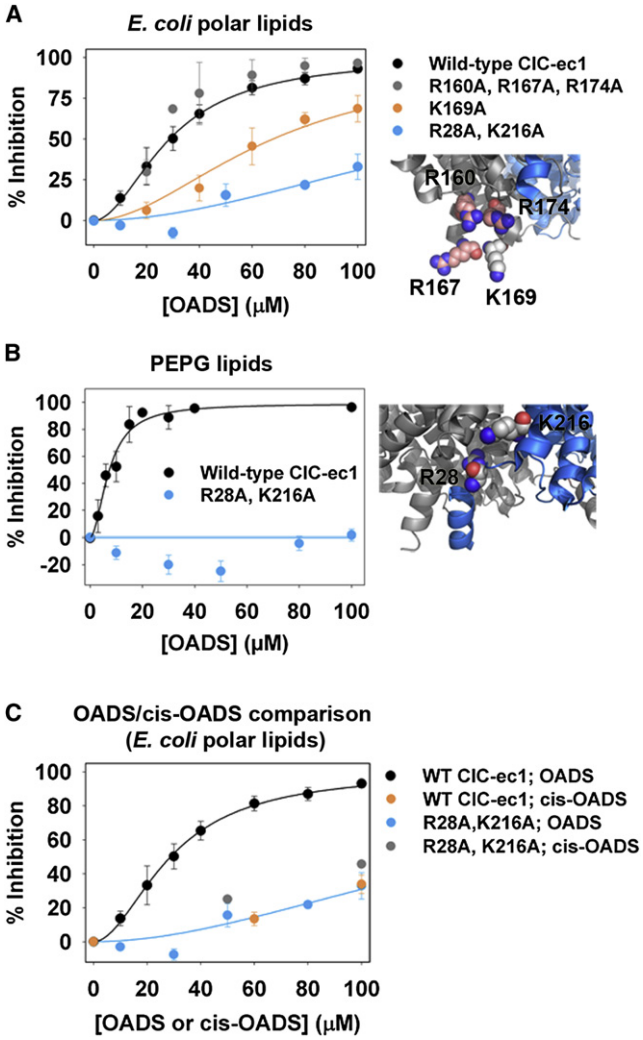

Figure 6. K169 and R28/K216 Constitute Functionally Relevant OADS Binding Sites

(A) Cl^- efflux assays reveal decreased sensitivity of K169 and R28/K216 mutants to OADS. Simultaneous mutation of three other cationic residues, R164, R160, and R172, all within 5 Å of K169 (inset), has no effect on inhibition. Assays were performed on liposomes formed from *E. coli* polar lipids. Error bars indicate SEM for three to seven experiments at each concentration.

(B) Inhibition of R28A/K216A by OADS is not detectable in Cl^- efflux assays with PE/PG liposomes. Data for WT are identical to that shown in Figure 1G. For R28A/K216A, error bars indicate SEM for five experiments at each concentration.

(C) In contrast to WT ClC-ec1, *cis*-OADS inhibits R28A/K216A just as potently as *trans*-OADS ("OADS"). Data are from Cl^- efflux assays on liposomes formed from *E. coli* polar lipids. Error bars indicate SEM for three to seven experiments at each concentration.

See also Figure S6.

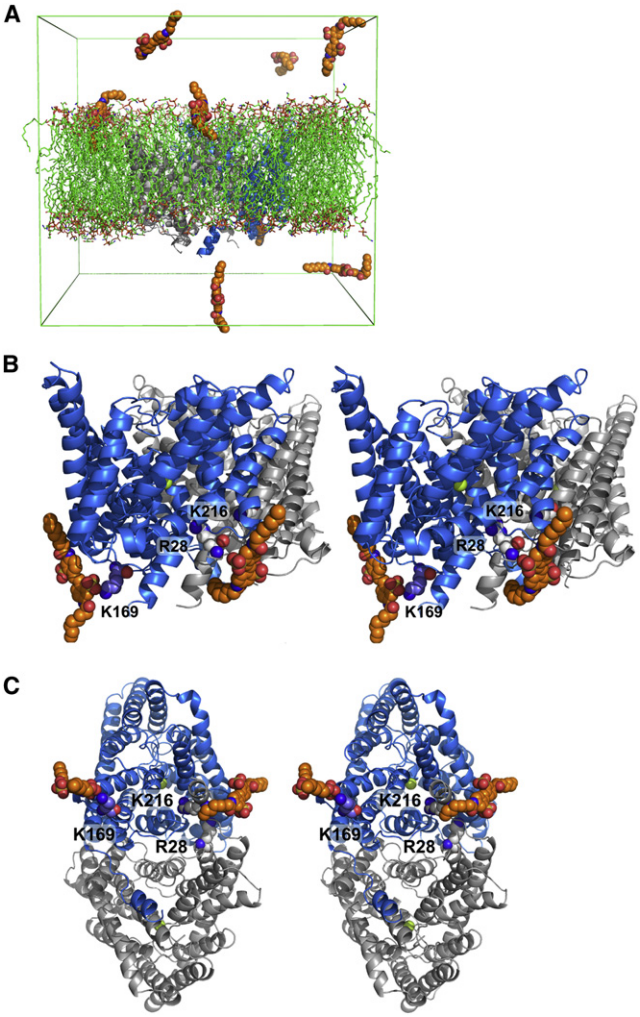

Figure 7. OADS Binding to ClC-ec1 at K169 and R28/K216 as Observed by Atomistic Molecular Dynamics Simulations

(A) Simulation system showing ClC-ec1 (blue/gray) in a lipid bilayer (green) with OADS (orange). Lower compartment corresponds to the intracellular side of the protein (see Experimental Procedures for more details of simulation system).

(B) Stereo view of ClC-ec1 showing that OADS associates with K169 through an ionic interaction and with R28/K216 through direct contact with the backbone of R28. For reference, chloride ions bound to the chloride permeation pathway of ClC-ec1 are shown space-filled in green.

(C) Rotated view, showing perspective from the cytoplasm.

charged residue in all of the known channels (Figure S5C). This observation suggests that OADS might be generally specific for CLC antiporters over channels.

The effect of cardiolipin (CLN) on both OADS potency (Figure 1G) and ClC-ec1 activity (Figure S1) suggests a functionally important CLN-protein interaction in ClC-ec1, perhaps similar to those observed in other proton-pumping proteins. In the cytochrome bc1 complex, for example, CLN is thought to serve as a local buffer capable of directly feeding protons into the ion permeation path (Haines and Dencher, 2002; Lange, et al., 2001). Consistent with CLN playing such a role in H^+ transfer by ClC-ec1, Cl^- efflux at pH 4.5 (slightly above the pH 4.0 used in the assays reported here) is robust in PE/CLN liposomes but severely reduced in PE/PG (in the absence of CLN) (Figure S1). OADS (Figure 1A) shares some basic structural features with CLN (including the presence of two central negative charges flanked by hydrocarbon chains). Thus, owing to the higher potency of OADS the absence of CLN (Figures 1E and 1G), it is tempting to speculate that OADS and CLN compete for a binding

site on ClC-ec1 (consistent with mechanism 3 in Figure 2A). A direct competition is unlikely, however, given that the R28A/K216A mutant has similar activity to wild-type ClC-ec1.

How does OADS binding impact ClC-ec1 function? The location of the OADS binding sites—away from the Cl^--permeation pathway (Figures 5A and 7B) —shows that OADS is not a classic "pore blocker." This conclusion is supported by mutagenesis of the intracellular vestibule leading to the Cl^--permeation pathway, because simultaneous neutralization of three charged residues in this region has no effect on inhibition by OADS (Figure S5A). We can further conclude that OADS does not indirectly cause occlusion of the chloride permeation pathway because ITC experiments reveal no significant effect on Cl^- binding to ClC-ec1 (Figure S6), Together, these results strongly suggest that OADS leaves the Cl^--permeation pathway intact and acts either by disrupting the H^+- permeation pathway or by hindering the transition between protein conformations involved in the Cl^-/H^+ transport cycle (hence slowing transport). The CLN influence on OADS affinity could thus arise from several possible mechanisms, including a specific interaction of CLN with the H^+-permeation pathway, a general membrane effect (Lundbaek, et al., 2010), and/or a propensity for ClC-ec1 to adopt a conformation more favorable to OADS binding without CLN present. If OADS does indeed act by "trapping" ClC-ec1 in a particular conformation, then OADS will be a powerful tool for investigating CLC conformational states that have been undetected by crystallography but glimpsed by NMR (Elvington, et al., 2009). In any case, our findings set the stage for inhibitor-driven investigations to elucidate function in this widespread and distinctive family of channels and transporters.

SIGNIFICANCE

CLC "chloride channel" proteins are essential for a wide variety of physiological processes and are distinctive in that only half of the CLC family members are true chloride channels, whereas the other half are chloride-proton antiporters. Investigations of this unique family of proteins thus hold promise for generating insight into fundamental mechanistic distinctions between channels and transporters. The study of CLCs has been hindered, however, by the lack of an established pharmacology. Here, we begin to fill this void by identifying and characterizing a compound that inhibits a CLC antiporter (ClC-ec1) and has little effect on a CLC channel (ClC-1). This molecule, OADS, was generated through combination of two generic anion-channel inhibitors that alone show no efficacy against ClC-ec1. OADS is a small-molecule inhibitor of the CLC antiporters that is both stable in solution and amenable to structural modification. These traits have allowed us to go beyond pure functional analysis to characterize details of inhibitor-protein binding. We first used a gramicidin-based assay to demonstrate that inhibition is due to protein binding rather than bilayer modification. This technology has broad applicability and vast potential for streamlining drug discovery efforts. We next used top-down mass spectrometry analysis and a photoaffinity-labeled OADS derivative to identify inhibitor binding sites, thus establishing the feasibility of these methods with large (50 kDa) integral membrane proteins. Finally, we used molecular dynamics simulations, mutagenesis, and activity assays to substantiate the relevance and specificity of the identified OADS-binding sites. The identification of these sites will aid in further development and refinement of next-generation CLC inhibitors.

EXPERIMENTAL PROCEDURES

Chemical Syntheses

OADS and its analogs were synthesized as described in the Supplemental Experimental Procedures.

Expression, Purification, and Reconstitution of ClC-ec1

ClC-ec1 containing a C-terminal polyhistidine tag was overexpressed in *E. coli*, purified, and reconstituted as described elsewhere (Accardi, et al., 2004; Walden, et al., 2007). Reconstituted liposomes were formed from either *E. coli* polar lipid extract or synthetic lipids (65% POPE/35% POPG or 65% POPE and 35% bovine cardiolipin), where POPE is 1-palmitoyl-2-oleoyl-*sn*-glycero-3-phosphoethanolamine and POPG is 1-palmitoyl-2-oleoyl-*sn*-glycero-3-phospho-(1'-*rac*-glycerol). All lipids were purchased from Avanti Polar Lipids.

Chloride Efflux Assays

Cl^- efflux assays were performed as previously described (Matulef, et al., 2008). The selected inhibitor was diluted from a 2–10 mM stock solution in H_2O to ClC-ec1-containing liposomes (in 300 mM KCl and 25 mM Na^+-citrate [pH 4.0]). An equal volume of H_2O was added to liposomes containing no inhibitor. OADS solubility is limited in salt solution (unlike in pure H_2O), and thus a final OADS concentration of no more than 100 μM was used in these experiments. (In contrast, PAL-OADS remains soluble up to millimolar concentrations in salt solution, and thus higher concentrations could be used in the mass spectrometry experiments described below.) Intra- and extravesicular solutions were equalized by freezing and thawing samples four times prior to extrusion through a 400 nm filter. Extravesicular solution was exchanged for low-chloride flux buffer (150 mM K_2SO_4, 50 mM KCl, and 25 mM Na^+-citrate [pH 4.0]) immediately prior to performing the experiment. Cl^- efflux was initiated by the addition of the potassium-selective ionophore valinomycin, which allows bulk electroneutral efflux of KCl, and was monitored using an extravesicular AgCl electrode. The turnover rate is defined as the initial rate of Cl^- efflux minus the initial efflux through control liposomes containing no ClC-ec1, divided by the number of ClC-ec1 molecules in the assay (Cl^- s^{-1} ClC-ec1^{-1}) (quantified as described by Walden et al., 2007, using an extinction coefficient of 0.85 cm^2/mg). Triton X-100 (0.1%) was added at the end of each assay as a control to reveal the total chloride.

Electrophysiological Recordings

Bilayer and patch-clamp recording were performed as described previously (Lísal and Maduke, 2009; Matulef and Maduke, 2005). See Supplemental Experimental Procedures for details.

Measurement of Bilayer Modification by OADS and Its Derivatives

Large unilamellar vesicles (LUVs) were made of 1,2-dierucoyl-sn-glycero-3-phosphocholine ($DC_{22:1}$ PC), loaded with the water-soluble fluorophore 8-aminonaphthalene-1,3,6-trisulfonic acid, disodium salt (ANTS) using a four-part process of sonication, freeze-thaw cycles, extrusion, and elution. The LUVs were doped with gramicidin (gA) from *B. brevis* and incubated for 20–24 hr at 12.5°C. Alternatively, gA containing vesicles were prepared by adding gA directly to the lipid. Both methods of vesicle preparation were subjected to the same four-step process and produced consistent control rates. The fluorescence produced by ANTS is quenched by thallium (Tl^+). Tl^+ and ANTS cross the bilayer slowly, whereas the conducting gA channels are very Tl^+ permeable, such that the Tl^+ influx rate (the rate of fluorescence quenching) becomes a measure of the number of conducting gA channels in the LUV membranes. To measure the fluorescence quench rate, the ANTS-loaded LUVs were mixed with the Tl^+ quencher using a stopped-flow spectrofluorometer (Applied Photophysics, SX.20), and the fluorescence quench rate was determined from a stretched-exponential fit to the fluorescence time course, as described

previously (Ingólfsson and Andersen, 2010, 2011). The stilbene derivatives are fluorescent, and background fluorescence was corrected by measuring the fluorescence time-course in the absence and presence of quencher, thus enabling correction for the background fluorescence and photobleaching of the OADS derivatives.

Binding Stoichiometry Determination by Mass Spectrum Analysis

Samples were analyzed by LC-MS on an Agilent 1100 binary pump HPLC and Thermo Fisher LTQ XL ion trap mass spectrometer. A 75 × 2.1 mm Zorbax 300SB-C3 Poroshell column was employed with initial conditions of 98% A (0.1% formic acid in water) and 2% B (0.1% formic acid in acetonitrile) ramped to 95% B in 10 min at a flow of 250 μl/min. Ionization was in positive ESI with mass range 400–2000 m/z. The injection volume was 10 μl of a 100× diluted in H_2O sample solution. Promass deconvolution software was used to plot the data as mass versus intensity.

Top-Down Mass-Spectrometry of Covalently Modified ClC-ec1

ClC-ec1 covalently modified with 500 μM PAL-OADS was precipitated with chloroform/methanol and dissolved in 100 μl of 90% formic acid (ACS grade, Fisher). The sample was immediately injected into a size-exclusion chromatography system previously equilibrated with $CHCl_3$/MeOH/1% aqueous formic acid (4:4:1, v/v), as previously described for lactose permease (a protein that weighs close to 50 kDa and has twelve transmembrane helices) (Whitelegge, et al., 1999). Column eluent was directed to a standard electrospray source (IonMax, Thermo Scientific) attached to a 7 Tesla hybrid linear ion trap Fourier-transform ion cyclotron resonance mass spectrometer (LTQ-FT Ultra, Thermo Scientific). The column (SW2000 XL, Tosoh Biosciences) was eluted with a flow rate of 250 μl/min, which was reduced to 5 μl/min immediately prior to elution of the protein peak 7 min into the run. This "peak parking" allows extended data collection on OADS/ClC-ec1 (10–90 min). The FT-MS was operated at 400,000 resolution (at 400 m/z) in order to achieve unit resolution of ^{13}C isotopomers. The mass spectrum was then transformed to the zero charge state using Xtract software (Xcaliber, Thermo Scientific). Collisionally activated dissociation (CAD) of the ion at m/z 1571 gave a complex mass spectrum that was analyzed using ProSightPC (Version 1.0; Thermo Scientific) to match CAD product ions to the primary structure of ClC-ec1 with 1 or 2 OADS molecules placed at different positions.

Molecular Dynamics Simulations

The ClC-ec1 dimer (PDB entry 1OTS) (Dutzler, et al., 2003) was inserted in a hydrated and equilibrated POPE/POPG(3:1) bilayer, set up with CHARMM-GUI (Jo, et al., 2008), using g_membed (Wolf, et al., 2010). The system contained 240 POPE lipids and 39 POPG lipids, 29509 TIP3P water molecules, and KCl salt at 150 mM concentration. The CHARMM36 force field was used together with the TIP3P water model (Klauda, et al., 2010). After energy minimization and equilibration for ~40 ns, eight molecules of OADS were inserted into the aqueous phase near the membrane. OADS was assumed to be in a dianionic state and the parameters for OADS were derived using CgenFF (Vanommeslaeghe, et al., 2010). See Supplemental Experimental Procedures for further details.

SUPPLEMENTAL INFORMATION

Supplemental Information includes six figures, two tables, and Supplemental Experimental Procedures and can be found with this article online at http://dx.doi.org/10.1016/j.chembiol.2012.09.017.

ACKNOWLEDGMENTS

We thank Martin Prieto for comments on the manuscript, David Kopfer for help with the parameterization of OADS, Hyun-Ho Lim and Chris Miller for help with crystallization attempts, Ricky Cheng for remedial Pymol and assistance with figures, and Thomas Jentsch for providing the hClC-1 DNA. This work was supported by the National Institutes of Health (Grants GM070773 to M.M. and GM021342 to O.S.A.), ARRA Supplements (Grants GM070773-05S1 to M.M. and GM021342-35S1 to O.S.A.), AHA (Grant 1137885-100-UADJU to M.M.), the Mathers Foundation (to M.M.), a Stanford University SPARK award (to M.M. and J.D.B.), Stanford University (to J.D.B.), a Research Corporation for Science Advancement Cottrell College Science Award (to K.M.), start-up funds from the University of San Diego (to K.M.), Scottish Universities Physics Alliance (to U.Z.), and the National Physical Laboratory (to U.Z.). Top-down mass spectrometry was performed on a 7T LTQ-FT Ultra purchased with National Institutes of Health support (Grant S10 RR023045). A.H. was supported by an Amgen Graduate Fellowship and a Roche Graduate Fellowship. S.P. was supported in part by a Summer Undergraduate Research Experience grant from the University of San Diego. K.T. was supported by a Stanford BioX Fellowship. T.C. was supported by the Stanford Institutes of Medicine Summer Research Program.

Received: May 31, 2012
Revised: August 29, 2012
Accepted: September 27, 2012
Published: November 21, 2012

REFERENCES

Accardi, A., and Miller, C. (2004). Secondary active transport mediated by a prokaryotic homologue of ClC Cl- channels. Nature *427*, 803–807.

Accardi, A., Kolmakova-Partensky, L., Williams, C., and Miller, C. (2004). Ionic currents mediated by a prokaryotic homologue of CLC Cl- channels. J. Gen. Physiol. *123*, 109–119.

Alper, S.L. (2009). Molecular physiology and genetics of Na+-independent SLC4 anion exchangers. J. Exp. Biol. *212*, 1672–1683.

Andersen, O.S. (2008). Perspectives on how to drug an ion channel. J. Gen. Physiol. *131*, 395–397.

Cabantchik, Z.I., and Greger, R. (1992). Chemical probes for anion transporters of mammalian cell membranes. Am. J. Physiol. *262*, C803–C827.

Chen, B., Nicol, G., and Cho, W.K. (2007). Role of calcium in volume-activated chloride currents in a mouse cholangiocyte cell line. J. Membr. Biol. *215*, 1–13.

Dormán, G., and Prestwich, G.D. (2000). Using photolabile ligands in drug discovery and development. Trends Biotechnol. *18*, 64–77.

Duan, D.D. (2011). The ClC-3 chloride channels in cardiovascular disease. Acta Pharmacol. Sin. *32*, 675–684.

Dutzler, R. (2006). The ClC family of chloride channels and transporters. Curr. Opin. Struct. Biol. *16*, 439–446.

Dutzler, R., Campbell, E.B., and MacKinnon, R. (2003). Gating the selectivity filter in ClsIC chloride channels. Science *300*, 108–112.

Elvington, S.M., Liu, C.W., and Maduke, M.C. (2009). Substrate-driven conformational changes in ClC-ec1 observed by fluorine NMR. EMBO J. *28*, 3090–3102.

Engh, A.M., and Maduke, M. (2005). Cysteine accessibility in ClC-0 supports conservation of the ClC intracellular vestibule. J. Gen. Physiol. *125*, 601–617.

Estévez, R., Schroeder, B.C., Accardi, A., Jentsch, T.J., and Pusch, M. (2003). Conservation of chloride channel structure revealed by an inhibitor binding site in ClC-1. Neuron *38*, 47–59.

Evanko, D.S., Zhang, Q., Zorec, R., and Haydon, P.G. (2004). Defining pathways of loss and secretion of chemical messengers from astrocytes. Glia *47*, 233–240.

Gradogna, A., and Pusch, M. (2010). Molecular pharmacology of kidney and inner ear CLC-K chloride channels. Front Pharmacol. *1*, 130.

Graves, A.R., Curran, P.K., Smith, C.L., and Mindell, J.A. (2008). The Cl-/H+ antiporter ClC-7 is the primary chloride permeation pathway in lysosomes. Nature *453*, 788–792.

Gupta, S.P., ed. (2011). Ion channels and their inhibitors 1Edition (Berlin, Germany: Springerlink).

Haines, T.H., and Dencher, N.A. (2002). Cardiolipin: a proton trap for oxidative phosphorylation. FEBS Lett. *528*, 35–39.

Huang, Z.M., Prasad, C., Britton, F.C., Ye, L.L., Hatton, W.J., and Duan, D. (2009). Functional role of CLC-2 chloride inward rectifier channels in cardiac sinoatrial nodal pacemaker cells. J. Mol. Cell. Cardiol. *47*, 121–132.

Ingólfsson, H.I., and Andersen, O.S. (2010). Screening for small molecules' bilayer-modifying potential using a gramicidin-based fluorescence assay. Assay Drug Dev. Technol. *8*, 427–436.

Ingólfsson, H.I., and Andersen, O.S. (2011). Alcohol's effects on lipid bilayer properties. Biophys. J. *101*, 847–855.

Jakobsen, P., and Horobin, R.W. (1989). Preparation and characterization of 4-acetamido-4′-isothiocyanostilbene-2,2′-disulfonic acid (SITS) and related stilbene disulfonates. Stain Technol. *64*, 301–313.

Jentsch, T.J. (2008). CLC chloride channels and transporters: from genes to protein structure, pathology and physiology. Crit. Rev. Biochem. Mol. Biol. *43*, 3–36.

Jeworutzki, E., López-Hernández, T., Capdevila-Nortes, X., Sirisi, S., Bengtsson, L., Montolio, M., Zifarelli, G., Arnedo, T., Müller, C.S., Schulte, U., et al. (2012). GlialCAM, a protein defective in a leukodystrophy, serves as a ClC-2 Cl(-) channel auxiliary subunit. Neuron *73*, 951–961.

Jo, S., Kim, T., Iyer, V.G., and Im, W. (2008). CHARMM-GUI: a web-based graphical user interface for CHARMM. J. Comput. Chem. *29*, 1859–1865.

Kasai, M., Kawasaki, T., and Yamaguchi, N. (1999). Regulation of the ryanodine receptor calcium release channel: a molecular complex system. Biophys. Chem. *82*, 173–181.

Kelleher, N.L. (2004). Top-down proteomics. Anal. Chem. *76*, 197A–203A.

Klauda, J.B., Venable, R.M., Freites, J.A., O'Connor, J.W., Tobias, D.J., Mondragon-Ramirez, C., Vorobyov, I., MacKerell, A.D., Jr., and Pastor, R.W. (2010). Update of the CHARMM all-atom additive force field for lipids: validation on six lipid types. J. Phys. Chem. B *114*, 7830–7843.

Lange, C., Nett, J.H., Trumpower, B.L., and Hunte, C. (2001). Specific roles of protein-phospholipid interactions in the yeast cytochrome bc1 complex structure. EMBO J. *20*, 6591–6600.

Li, L., Ma, K.T., Zhao, L., Si, J.Q., Zhang, Z.S., Zhu, H., and Li, J. (2008). Niflumic acid hyperpolarizes smooth muscle cells via calcium-activated potassium channel in spiral modiolar artery of guinea pigs. Acta Pharmacol. Sin. *29*, 789–799.

Liantonio, A., Picollo, A., Carbonara, G., Fracchiolla, G., Tortorella, P., Loiodice, F., Laghezza, A., Babini, E., Zifarelli, G., Pusch, M., and Camerino, D.C. (2008). Molecular switch for CLC-K Cl- channel block/activation: optimal pharmacophoric requirements towards high-affinity ligands. Proc. Natl. Acad. Sci. USA *105*, 1369–1373.

Liantonio, A., Gramegna, G., Camerino, G.M., Dinardo, M.M., Scaramuzzi, A., Potenza, M.A., Montagnani, M., Procino, G., Lasorsa, D.R., Mastrofrancesco, L., et al. (2012). In-vivo administration of CLC-K kidney chloride channels inhibitors increases water diuresis in rats: a new drug target for hypertension? J. Hypertens. *30*, 153–167.

Lin, C.W., and Chen, T.Y. (2003). Probing the pore of ClC-0 by substituted cysteine accessibility method using methane thiosulfonate reagents. J. Gen. Physiol. *122*, 147–159.

Lísal, J., and Maduke, M. (2009). Review: proton-coupled gating in chloride channels. Philos. Trans. R. Soc. Lond. B Biol. Sci. *364*, 181–187.

Lossin, C., and George, A.L., Jr. (2008). Myotonia congenita. Adv. Genet. *63*, 25–55.

Lundbaek, J.A., Collingwood, S.A., Ingólfsson, H.I., Kapoor, R., and Andersen, O.S. (2010). Lipid bilayer regulation of membrane protein function: gramicidin channels as molecular force probes. J. R. Soc. Interface *7*, 373–395.

Maduke, M., Pheasant, D.J., and Miller, C. (1999). High-level expression, functional reconstitution, and quaternary structure of a prokaryotic ClC-type chloride channel. J. Gen. Physiol. *114*, 713–722.

Matulef, K., and Maduke, M. (2005). Side-dependent inhibition of a prokaryotic ClC by DIDS. Biophys. J. *89*, 1721–1730.

Matulef, K., Howery, A.E., Tan, L., Kobertz, W.R., Du Bois, J., and Maduke, M. (2008). Discovery of potent CLC chloride channel inhibitors. ACS Chem. Biol. *3*, 419–428.

Miller, C. (1983). Integral membrane channels: studies in model membranes. Physiol. Rev. *63*, 1209–1242.

Miller, C. (2006). ClC chloride channels viewed through a transporter lens. Nature *440*, 484–489.

Nighot, P.K., Moeser, A.J., Ryan, K.A., Ghashghaei, T., and Blikslager, A.T. (2009). ClC-2 is required for rapid restoration of epithelial tight junctions in ischemic-injured murine jejunum. Exp. Cell Res. *315*, 110–118.

Picollo, A., and Pusch, M. (2005). Chloride/proton antiporter activity of mammalian CLC proteins ClC-4 and ClC-5. Nature *436*, 420–423.

Planells-Cases, R., and Jentsch, T.J. (2009). Chloride channelopathies. Biochim. Biophys. Acta *1792*, 173–189.

Ratté, S., and Prescott, S.A. (2011). ClC-2 channels regulate neuronal excitability, not intracellular chloride levels. J. Neurosci. *31*, 15838–15843.

Robertson, J.L., Kolmakova-Partensky, L., and Miller, C. (2010). Design, function and structure of a monomeric ClC transporter. Nature *468*, 844–847.

Robinette, D., Neamati, N., Tomer, K.B., and Borchers, C.H. (2006). Photoaffinity labeling combined with mass spectrometric approaches as a tool for structural proteomics. Expert Rev. Proteomics *3*, 399–408.

Scheel, O., Zdebik, A.A., Lourdel, S., and Jentsch, T.J. (2005). Voltage-dependent electrogenic chloride/proton exchange by endosomal CLC proteins. Nature *436*, 424–427.

Thompson, C.H., Olivetti, P.R., Fuller, M.D., Freeman, C.S., McMaster, D., French, R.J., Pohl, J., Kubanek, J., and McCarty, N.A. (2009). Isolation and characterization of a high affinity peptide inhibitor of ClC-2 chloride channels. J. Biol. Chem. *284*, 26051–26062.

Vanommeslaeghe, K., Hatcher, E., Acharya, C., Kundu, S., Zhong, S., Shim, J., Darian, E., Guvench, O., Lopes, P., Vorobyov, I., and Mackerell, A.D., Jr. (2010). CHARMM general force field: a force field for drug-like molecules compatible with the CHARMM all-atom additive biological force fields. J. Comput. Chem. *31*, 671–690.

Venglarik, C.J., Singh, A.K., and Bridges, R.J. (1994). Comparison of -nitro versus -amino 4,4′-substituents of disulfonic stilbenes as chloride channel blockers. Mol. Cell. Biochem. *140*, 137–146.

Verkman, A.S., and Galietta, L.J. (2009). Chloride channels as drug targets. Nat. Rev. Drug Discov. *8*, 153–171.

Walden, M., Accardi, A., Wu, F., Xu, C., Williams, C., and Miller, C. (2007). Uncoupling and turnover in a Cl-/H+ exchange transporter. J. Gen. Physiol. *129*, 317–329.

Whitelegge, J.P., le Coutre, J., Lee, J.C., Engel, C.K., Privé, G.G., Faull, K.F., and Kaback, H.R. (1999). Toward the bilayer proteome, electrospray ionization-mass spectrometry of large, intact transmembrane proteins. Proc. Natl. Acad. Sci. USA *96*, 10695–10698.

Wolf, M.G., Hoefling, M., Aponte-Santamaría, C., Grubmüller, H., and Groenhof, G. (2010). g_membed: Efficient insertion of a membrane protein into an equilibrated lipid bilayer with minimal perturbation. J. Comput. Chem. *31*, 2169–2174.

Woodhull, A.M. (1973). Ionic blockage of sodium channels in nerve. J. Gen. Physiol. *61*, 687–708.

Yan, Q., ed. (2010). Membrane transporters in drug discovery and development (New York, NY: Humana).

Zhang, X.D., and Chen, T.Y. (2009). Amphiphilic blockers punch through a mutant CLC-0 pore. J. Gen. Physiol. *133*, 59–68.

Zhao, Q., Wei, Q., He, A., Jia, R., and Xiao, Y. (2009). CLC-7: a potential therapeutic target for the treatment of osteoporosis and neurodegeneration. Biochem. Biophys. Res. Commun. *384*, 277–279.